Implicit sequential filtering

S. Danilov, S. Juricke*, K. Nowak, D. Sidorenko, Q. Wang,
AWI, Bremerhaven
*GEOMAR, Kiel

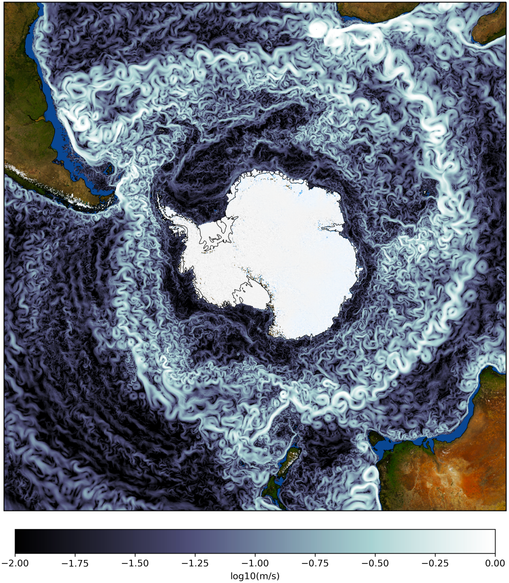

Figure: Snapshot of $|\mathbf{u}|$ at $z = -100$ m in the SO.

Sequential filtering and spectra:

$$\overline{\phi}_\ell(\mathbf{x}) = G_\ell * \phi(\mathbf{x})$$

$$\overline{\mathcal{E}}_\ell(\mathbf{x}) = \overline{\phi}_\ell(\mathbf{x})^2$$

Aluie et al. 2018, Sadek and Aluie 2018:

$$k_\ell = 1/\ell$$

$$\overline{E}(\mathbf{x}, k_\ell) = \partial\overline{\mathcal{E}}_\ell/\partial k_\ell$$

The spectrum $\overline{E}(\mathbf{x}, k_\ell)$ is available at all locations $\mathbf{x}$.

Regular mesh is needed for efficient implementation

Coarsening on general (varying or unstructured) meshes

Solve

$$(1+\gamma(-\ell^2\Delta)^n)\overline{\phi}_\ell = \phi, \quad \mathbf{x}\in D, \quad \partial\overline{\phi}_\ell/\partial\mathbf{n} = 0 \text{ on } \partial D. \qquad (1)$$

How does it work? Consider the Fourier-transform for $n = 1$:

$$\hat{\overline{\phi}}_\ell(k) = \hat{G}_\ell(k)\hat{\phi}(k) = \frac{\hat{\phi}(k)}{1+\gamma\ell^2 k^2},$$

k is the wavenumber, $\hat{\phi}(k)$ is Fourier transformed ϕ, and $\hat{G}_\ell(k)$ is the Fourier transform of the convolution kernel; γ is a tuning parameter.

$\overline{\phi}_\ell$ is a low pass version of ϕ

Coarsening on general (varying or unstructured) meshes

Discrete Laplacian operator

- Can be constructed for any mesh
- In spherical or flat geometry
- It can be constructed for scalar and vector data
- It depends only on the nearest neighbors — easy to parallelize
- An iterative solver (and good preconditioner for $n \geq 2$) are needed

Elementary theory

Let E_k be the Fourier energy spectrum,

$$E = \int_0^\infty E_k dk,$$

Let

$$\overline{\mathcal{E}}_\ell = \frac{\int \overline{\mathcal{E}}_\ell(\mathbf{x}) d\mathbf{x}}{\int d\mathbf{x}}$$

Then:

$$\overline{\mathcal{E}}_\ell = \int_0^\infty |\hat{G}_\ell|^2 E_k dk = \int_0^\infty \frac{E_k dk}{(1+\gamma\ell^2 k^2)^2}.$$

Elementary theory

We can introduce a spectrum

$$\overline{E}(k_\ell) = \partial\overline{\mathcal{E}}_\ell/\partial k_\ell = \int_0^\infty \frac{\partial|\hat{G}_\ell|^2}{\partial k_\ell} E_k dk = \int_0^\infty \frac{4\gamma k^2/k_\ell^2}{(1+\gamma k^2/k_\ell^2)^3} E_k \frac{dk}{k_\ell}.$$

$\overline{E}(k_\ell)dk_\ell$ is the energy between k_ℓ and $k_\ell + dk_\ell$.

The form-factor

$$F = \frac{\partial|\hat{G}_\ell|^2}{\partial k_\ell}$$

determines the correspondence between E_k and $\overline{E}(k_\ell)$.

It is a function of k, and its peak will be at some $k_{peak}(\gamma, k_\ell)$.

Comparison with explicit convolution kernels

A box convolution kernel with width ℓ in the k-space is

$$\hat{G}_\ell(k) = \frac{\sin(k\ell/2)}{(k\ell/2)}.$$

As $z = k\ell \to 0$, $\hat{G}_\ell(k) \approx 1 - z^2/24$. For a Gaussian filter this leads to

$$\hat{G}_\ell(k) = \exp(-k^2\ell^2/24).$$

For implicit harmonic filter this leads to $\gamma = 1/24$,

$$\hat{G}_\ell(k) = \frac{1}{1 + k^2\ell^2/24}.$$

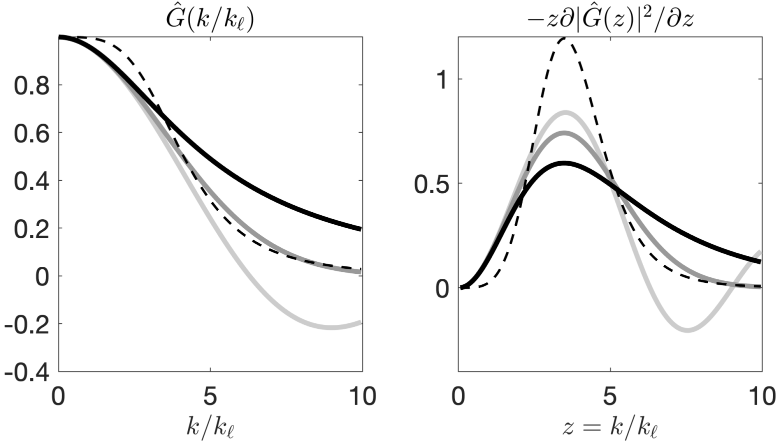

Figure: Convolution kernels (left) and the dimensionless form-factor $k_\ell \partial|\hat{G}_\ell(k)|^2/\partial k_\ell$ (right) as functions of $z = k/k_\ell$. Shown are the box kernel (light gray), Gaussian kernel (gray), implicit second-order kernel with $\gamma = 1/24$ (black) and implicit fourth-order kernel ($n = 2$) with $\gamma = 1/288$ (dashed).

High pass versus low pass

$$\overline{\psi}_\ell = \phi(\mathbf{x}) - \overline{\phi}_\ell(\mathbf{x})$$

$$\overline{\mathcal{E}}_\ell^H = \overline{\psi}_\ell(\mathbf{x})^2,$$

$$\overline{E}(\mathbf{x}, k_\ell) = -\partial\overline{\mathcal{E}}_\ell^H/\partial k_\ell$$

Form-factor

$$F^H = -\frac{\partial}{\partial k_\ell}|1 - G(k, k_\ell)|^2 = \frac{4\gamma n}{k_\ell}\frac{(k/k_\ell)^{4n}}{(1+\gamma(k/k_\ell)^{2n})^3}.$$

Higher power of k as $k/k_\ell \to 0$! Steeper slopes can be recovered.

Matrix problem

$$\mathsf{S}_{vv'}\overline{\phi}_{v'} = A_v \phi_v$$

Summation over repeating index v' is implied. A_v area related to v

$$\mathsf{S}_{vv'} = A_v \mathsf{I}_{vv'} - (1/2) A_v \mathsf{L}_{vv'}$$

$\mathsf{I}_{vv'}$ the identity matrix, $\mathsf{L}_{vv'}$ the matrix of discrete Laplacian.

$\mathsf{S}_{vv'}$ is a positive symmetric matrix $\Rightarrow$ CG solver.

The choice $\gamma = 1/2$ ensures the agreement of k_ℓ and k.

Illustrations

A regular quadrilateral mesh, $L_x = L_y = 1024$ km, side $a = 4$ km.
Take $\phi(\mathbf{x}) = \mathrm{rand}$, FT $\phi \to \hat{\phi}(\mathbf{k})$, make red $\hat{\phi}(\mathbf{k}) \to \hat{\phi}(\mathbf{k})K^{(\alpha+1)/2}$, $K = |\mathbf{k}|$, inverse FT. $\Rightarrow E_K \sim K^{-\alpha}$.

Triangular meshes

- Q: Split quads into triangle, use original data
- E: Uniform Equilateral mesh, interpolated data
- U: An unstructured mesh with resolution varying two-fold , interpolated data

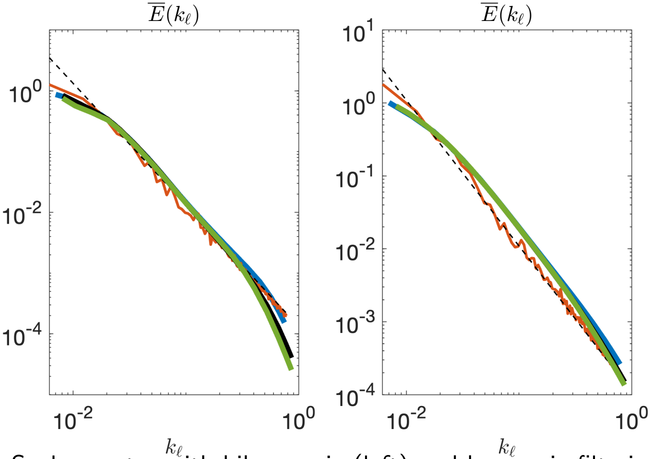

Figure: Scale spectra with biharmonic (left) and harmonic filtering (right). Fourier spectrum (red), scale spectra on mesh Q (no interpolation, blue), regular equilateral mesh (solid black, mesh E) and on an irregular unstructured mesh (green, mesh U), k_ℓ in cycle/km.

Peak detection

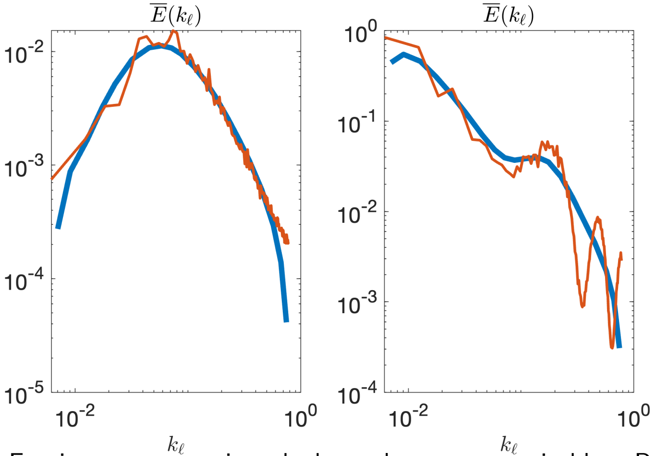

Figure: Fourier spectra are in red, the scale spectra are in blue. Peaks can be missed or masked if they are narrow and/or there are neighboring intervals with high spectral density.

Harmonic filter vs explicit box-type filter

We use a box-type filter with the kernel

$$G(\mathbf{x}) = A(1 - \tanh(c(|\mathbf{x}| - 1.75/k_\ell)/a)),$$

where A is the normalization constant selected so as to ensure that $\int G(\mathbf{x})d\mathbf{x} = 1$, a is the (fixed) mesh cell size, $c = 1.3$ is a numerical factor controlling the sharpness of the box filter transition, and $1.75/k_\ell$ is equivalent to the scale $\ell_{\rm box}/2$

Harmonic filter vs explicit box-type filter

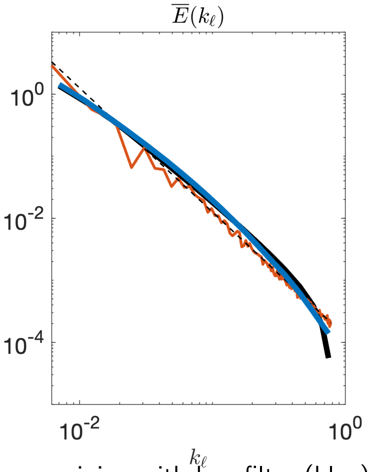

Figure: Explicit coarse-graining with box filter (blue) and Laplacian-based filter (solid black). The Fourier spectrum is in red, and the dashed line corresponds to the slope of -2.

Vector fields

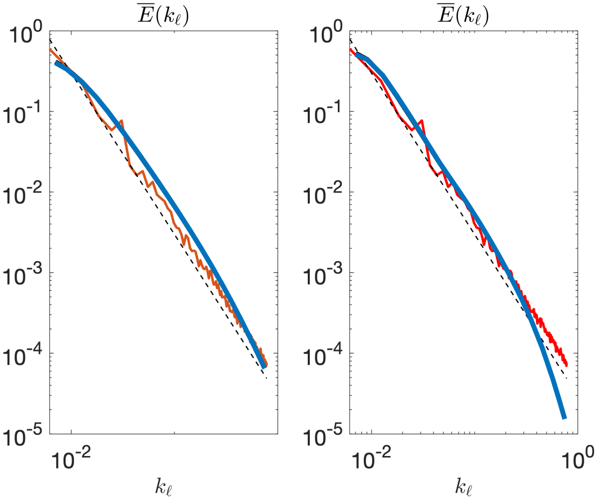

Figure: Scale spectra of KE, harmonic (left) and biharmonic (right) filters, full metric terms (blue), no metric terms (black).

Filtering on strongly nonuniform meshes

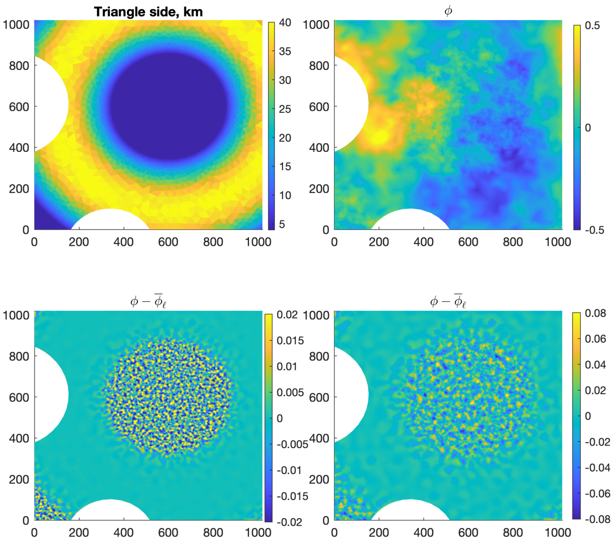

Figure: Mesh resolution, a realization, high-pass filtering with biharmonic and harmonic filters.

High-pass filter, 1 km Arctic mesh

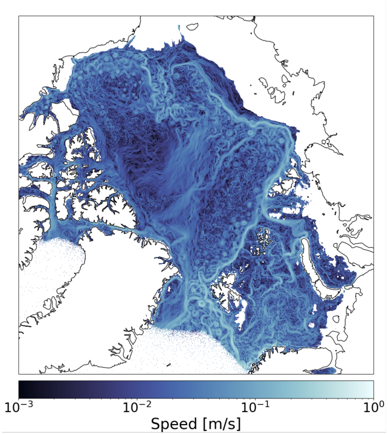

Figure: A snapshot of velocity field at 70m, full and high-pass at 100 km.

Harmonic vs. biharmonic, 1 km Arctic mesh

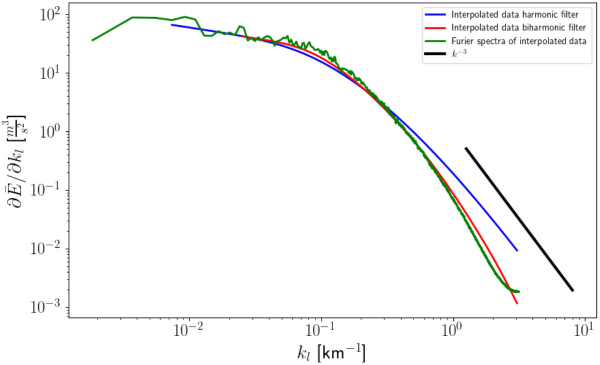

Figure: A snapshot of velocity field at 70m, full and high-pass at 100 km.

Discussions

- Convergence deteriorates if n is increased and ℓ approaches the size of domain
- a CG solver may need $\sim 10^4$ iterations, preconditioners are vital
- A python-based JAX accelerated version takes a few minutes on GPUs on meshes with about 10M wet surface vertices (larger than ORCA 1/12)
- Can be applied to cross-spectra, e.g. $g_\ell = w_\ell b_\ell$ or energy transfers between scales
- Spatial patterns of $\mathcal{E}_{\ell_1}(\mathbf{x}) - \mathcal{E}_{\ell_2}(\mathbf{x})$ carry more information than spectra.

Conclusions

- Coarsening based on implicit filters is an efficient way to work on native meshes;
- The method works with scalar or vertex data in flat or spherical geometry;
- High-order (biharmonic, three-harmonic, ...) filters are needed for better scale selectivity;